Ultrahigh-Resolution γ-Ray Spectroscopy of ^{156}Gd: A Test of Tetrahedral Symmetry

M. Jentschel,[1] W. Urban,[1,2] J. Krempel,[1] D. Tonev,[3] J. Dudek,[4] D. Curien,[4] B. Lauss,[5] G. de Angelis,[6] and P. Petkov[3]

[1]*Institut Laue-Langevin, 6 rue Jules Horowitz, BP 156, F-38042 Grenoble, France*
[2]*Faculty of Physics, University of Warsaw, ul. Hoża 69, PL-00-681 Warsaw, Poland*
[3]*Institute for Nuclear Research and Nuclear Energy, BAS, BG-1784 Sofia, Bulgaria*
[4]*Departement de Recherches Subatomiques, Institut Pluridisciplinaire Hubert Curien, DRS-IPHC, 23 rue du Loess, BP 28, F-67037 Strasbourg, France*
[5]*Paul Scherrer Institut, CH-5232 Villigen-PSI, Switzerland*
[6]*Laboratori Nazionali di Legnaro, I-35020 Legnaro, Italy*

(Received 26 February 2010; published 4 June 2010)

Tetrahedral symmetry in strongly interacting systems would establish a new class of quantum effects at subatomic scale. Excited states in ^{156}Gd that could carry the information about the tetrahedral symmetry were populated in the ^{155}Gd$(n,\gamma)^{156}$Gd reaction and studied using the GAMS4/5 Bragg spectrometers at the Institut Laue-Langevin. We have identified the $5_1^- \rightarrow 3_1^-$ transition of 131.983(12) keV in ^{156}Gd and determined its intensity to be $1.9(3)x10^{-6}$ per neutron capture. The lifetime $\tau = 220^{+180}_{-30} fs$ of the 5_1^- state in ^{156}Gd has been measured using the GRID technique. The resulting $B(E2) = 293^{+61}_{-134}$Weisskopf unit rate of the 131.983 keV transition provides the intrinsic quadrupole moment of the 5_1^- state in ^{156}Gd to be $Q_0 = 7.1^{+0.7}_{-1.6}$ b. This large value, comparable to the quadrupole moment of the ground state in ^{156}Gd, gives strong evidence against tetrahedral symmetry in the lowest odd-spin, negative-parity band of ^{156}Gd.

DOI: 10.1103/PhysRevLett.104.222502 PACS numbers: 21.10.Tg, 23.20.−g, 27.60.+j, 27.70.+q

In nuclear structure it is of particular interest to formulate stability criteria by generalizing the concept of shells and ''magic numbers'' from spherical, SO(3)-symmetric nuclei to other symmetries. In Refs. [1–4] a new theory has been laid out stating that: (i) A sufficiently rich in symmetry subgroup, $G \subset \mathrm{SO}(3)$, may give rise to nonspherical shell gaps comparable with those in spherical nuclei, and (ii) The chances for this mechanism to produce large gaps (thus strong stability) increase when the numbers of the group's irreducible representations and their dimensions are large. The tetrahedral point-group symmetry is one of the favored candidates.

The existence of such symmetries in *atomic nuclei* would represent a qualitatively new result in physics. In molecules the nontrivial point-group symmetries are common as a result of electromagnetic interaction. Such symmetries in nuclei, with a compact distribution of elementary particles governed by strong interactions, would represent a new class of physical phenomena.

A negative-parity band in the nucleus ^{156}Gd is predicted to be a favorable candidate to manifest tetrahedral symmetry [2]. The first direct investigation was carried out without any firm conclusion [5]. In a more recent work [6] the quadrupole moments of ^{160}Yb and ^{154}Gd have been deduced from band mixing calculations and found to be inconsistent with the tetrahedral symmetry assumption. In this Letter we report on a direct test of tetrahedral symmetry in the lowest negative-parity band in ^{156}Gd using the ultra-high-resolution γ-ray spectrometers GAMS.

Tetrahedral shapes correspond to a nonaxial octupole deformation (Y_{32}) with a vanishing quadrupole deformation [1]. In a nucleus with tetrahedral shape a rotational negative-parity band would have vanishing intraband $E2$ transitions, especially at the bottom of the band, where the angular-momentum-induced quadrupole moment is small. The lowest odd-spin, negative-parity rotational band in ^{156}Gd, interpreted previously as an octupole band [7,8], may indicate a tetrahedral symmetry in this nucleus because the intraband $E2$ transitions are absent at the bottom of the band. The partial excitation scheme of ^{156}Gd is shown in Fig. 1, following a recent compilation [9]. More properties of γ transitions in ^{156}Gd are reported in Tables I and II.

The neutron-rich lanthanides where axial octupole deformation (Y_{30}) has been predicted and [14] found experimentally. The strongest octupole effects have been found in $^{144}_{56}\mathrm{Ba}_{88}$ [15] and $^{150}_{62}\mathrm{Sm}_{88}$ [16], where negative-parity, $K^\pi = 0^-$, octupole band and the positive-parity, ground-state band intertwine into the so-called alternating-parity band. In such band the positive- and negative-parity levels are linked by strong $E1$ transitions, with $B(E1)$ values increased up to 10^{-2} W.u. (Weisskopf unit), a few orders of magnitude higher than the average for $B(E1)$ values in nuclei. In the alternating-parity band γ intensities of the $E1$ and $E2$ transitions are comparable and the $B(E2)$ rates between the negative-parity levels are similar to or larger than the $B(E2)$ rates between the positive-parity levels [17,18].

This picture changes above neutron number $N = 90$, where the quadrupole deformation increases and the energies of the in-band $E2$ transitions become significantly lower. As a consequence, $I_\gamma(E1)/I_\gamma(E2)$ intensity ratios increase dramatically, resulting in the nonobservation of the $E2$ branches, for which γ intensities fall below the limit

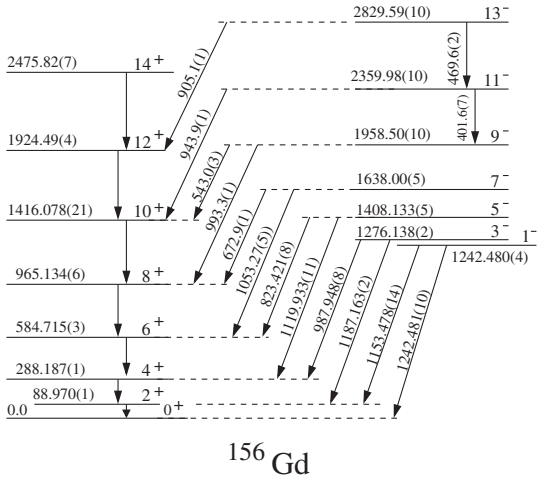

FIG. 1. Partial level scheme of ^{156}Gd, data from [9]. The ground-state band (positive parity) and the band candidate to represent tetrahedral symmetry (negative parity) are shown. Transition and level energies are given in keV.

of most γ-spectroscopy detection techniques. A good example is the negative-parity band in ^{156}Gd where the in-band $E2$ decays have not been observed for levels with spin $I < 11$ [9].

Similar negative-parity bands were found in several Gd nuclei, as shown in Fig. 2(a). Figure 2(b) shows excitation energies in the negative-parity bands of the $N = 92$ isotones. In both pictures the negative-parity band of ^{156}Gd fits well a smooth trend, suggesting that this band is of the same origin as the other negative-parity bands shown.

The interpretations based on axial octupole deformation [7,8] as well as the IBA-1 calculations described in [19] reproduce well the level schemes and the $B(E1)$ and $B(E2)$ values of the rotational bands observed in rare earth nuclei and, in particular, the negative-parity band of ^{156}Gd. Those interpretations are clearly different from the tetrahedral description (nonaxial octupole character) [2]. Since both approaches describe well excitation energies of the band, the only way to verify the hypothesis of the tetrahedral symmetry is to measure the degree of quadrupole collectivity in the octupole band. It is expected to be as high as in the ground-state band for the $K = 0$ octupole band [1], while it is predicted to be very low or vanishing for the tetrahedral band ($K = 2$) [2].

TABLE I. Energies, E_γ and intensities, I_γ of γ lines of ^{156}Gd.

Transition $I_i^\pi \to I_f^\pi$	E_γ (keV) Ref. [9]	E_γ (keV) this work	I_γ (per 10^4 capt.)
$3_1^- \to 4_1^+$	987.948(8)	987.9440(5)	
$5_1^- \to 4_1^+$	1119.933(11)	1119.9335(14)	90(7)[b]
$5_1^- \to 6_1^+$	823.421(8)		27.1(14)[b]
$5_1^- \to 3_1^-$		131.983(12)	0.019(3)[a]

[a]As measured in this work.
[b]As reported in Ref. [10].

The aim of the present work is the investigation of branching ratios and electromagnetic decay rates for the critical 5^- member of the negative-parity band in ^{156}Gd. This information should either prove, or disprove, the existence of tetrahedral deformation in this band.

The experiment described in this work exploited the ultrahigh resolution of the γ-ray spectrometers GAMS4 [20] and GAMS5 at the high flux reactor of the Institut Laue-Langevin (ILL). The GAMS4 spectrometer is equipped with flat crystals yielding a high relative energy resolution of $\Delta E/E \simeq 10^{-6}$ but a low effective solid angle of 10^{-11}. Its unique high resolution allows one to determine nuclear state lifetimes using the GRID technique [21,22]. Furthermore, the spectrometer is capable of measuring absolute energies. The GAMS5 spectrometer was equipped with curved crystals in DuMond diffraction geometry. This increases the solid angle to 10^{-7} for the price of a lower energy resolution ($\Delta E/E \simeq 10^{-4}$ at 100 keV).

TABLE II. The $B(E1)$ and $B(E2)$ rates for selected transitions in ^{156}Gd and its neighbor nuclei. We have evaluated $B(E\lambda)$ values for the 5_1^- level in ^{158}Gd taking its lifetime $\tau = 0.46^{+0.36}_{-0.11}$, as recommended in Ref. [13], estimating error bars in the same way as done in this work for the lifetime of the 5_1^- level in ^{156}Gd. We note that in Ref. [12] unreasonable small error bars are quoted for $B(E\lambda)$decay rates of the 5_1^- level in ^{158}Gd.

Nucleus	Transition $I_i^\pi \to I_f^\pi$	E_γ (keV)	$B(E2)$ (W.u.)	$B(E1)$ (W.u. $\times 10^{-3}$)
^{154}Sm	$2_1^+ \to 0_1^+$	123.0706	157(1)[c]	
	$4_1^+ \to 2_1^+$	247.9288	245(9)[c]	
	$3_1^- \to 2_1^+$	930.37		0.80(11)[c]
	$3_1^- \to 4_1^+$	645.50		0.92(13)[c]
^{154}Gd	$2_1^+ \to 0_1^+$	123.0706	157(1)[c]	
	$4_1^+ \to 2_1^+$	247.9288	245(9)[c]	
^{156}Gd	$2_1^+ \to 0_1^+$	88.970	187(5)[b]	
	$4_1^+ \to 2_1^+$	199.219	263(5)[b]	
	$3_1^- \to 2_1^+$	1187.1631		0.98(21)[b]
	$3_1^- \to 4_1^+$	987.9440		0.77(16)[b]
	$5_1^- \to 4_1^+$	1119.9335		$0.85^{+.19}_{-.38}$[a]
	$5_1^- \to 6_1^+$	823.421		$0.64^{+.14}_{-.29}$[a]
	$5_1^- \to 3_1^-$	131.983	293^{+61}_{-134}[a]	
^{158}Gd	$2_1^+ \to 0_1^+$	79.5132	198(6)[d]	
	$4_1^+ \to 2_1^+$	181.943	289(5)[d]	
	$3_1^- \to 2_1^+$	962.122		0.33(1)[d]
	$3_1^- \to 4_1^+$	780.183		0.29(8)[d]
	$5_1^- \to 4_1^+$	915.03		$0.77^{+.23}_{-.34}$[e]
	$5_1^- \to 6_1^+$	637.469		$0.60^{+.20}_{-.27}$[e]
	$5_1^- \to 3_1^-$	134.848	355^{+103}_{-155}[e]	

[a]Data from this work.
[b]Data from Ref. [9].
[c]Data from Ref. [11].
[d]Data from Ref. [12].
[e]Data from Ref. [13].

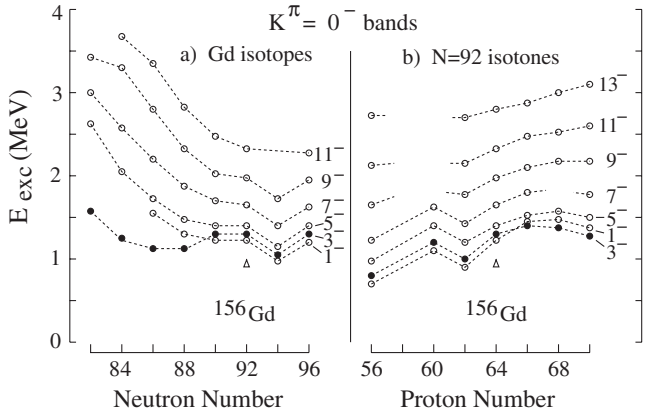

FIG. 2. Excitation energies in $K^{\pi} = 0^-$ octupole bands in neutron-rich lanthanides, relative to the ground state [18].

Because of its focusing diffraction geometry it requires small samples (a few tens of milligrams). Thanks to the diffraction process, the detectors at GAMS have a very small background rate and can detect γ transitions with a dynamical range of 10^5. This, together with its good energy resolution make the spectrometer a unique tool for the search for very weak transitions.

Using the GRID technique [21] the lifetimes of the 5_1^- and 3_1^- levels in ^{156}Gd were measured. Three samples of 5 grams of Gd_2O_3 powder with natural isotopic composition were inserted into the beam tube of the ILL reactor. The nuclear state lifetime was determined from the measured Doppler broadening of a transition, where corrections for instrument response and thermal broadening have been subtracted. The instrument response function was measured using third order nondispersive scans of the 944.191 keV transition in ^{158}Gd. The lifetime of the 2^- level at 1023.697 keV in ^{158}Gd is known to be >3.5 ps (typical slowing down times are about 200 fs). Therefore, the dispersive third order scans of the 944.191 keV transition allowed us to extract the nuclear thermal velocity.

The lifetime measurement of the 3_1^- state in ^{156}Gd used the Doppler broadening obtained from the 987.948 keV transition in third order dispersive geometry. As already discussed in detail in [10,22] the unknown feeding has a substantial influence on the extracted lifetime value. In order to take this into account the fraction of unknown feeding was simulated by a two step cascade. The energy and lifetime of an intermediate level, between capture and 3_1^- state, were varied and for each combination a lifetime value together with a χ^2 was obtained. The lifetime value with the lowest χ^2 was adopted and the respective error estimate performed. This yielded a lifetime of $\tau = 0.303^{+0.073}_{-0.075}$ ps in good agreement with $\tau = 0.200^{+0.050}_{-0.070}$ ps published in [10].

Subsequently, the Doppler broadening of the 823.421 keV transition corresponding to the $5_1^- \rightarrow 6_1^+$ de-excitation in ^{156}Gd was measured. The impact of the unknown feeding of the 5^- state on the value of the lifetime was investigated again by statistical χ^2 analysis as for the 3_1^- state and gave a lifetime of $\tau = 0.220^{+0.180}_{-0.030}$ ps.

In the next step we have focussed on the measurement of the $5_1^- \rightarrow 3_1^-$ transition. In a previous measurement using the bent crystal spectrometers GAMS2/3 [10] the $5_1^- \rightarrow 3_1^-$ transition was not observed, probably because of a limited count rate. We note that the focus of Ref. [10] was to measure a wide energy range from 50 keV up to 1 MeV. Limiting our experiment to scan only in a small energy region has allowed us to increase the statistical sensitivity.

The assignment of the $5_1^- \rightarrow 3_1^-$ transition to the negative-parity band can be facilitated by a precise determination of the energy difference between the 5_1^- and the 3_1^- levels. This was done using GAMS4 for measuring precisely the $5_1^- \rightarrow 4_1^+$ and the $3_1^- \rightarrow 4_1^+$ transitions. As the lattice spacing of the GAMS4 crystals is known and the angle interferometers can be absolutely calibrated [20], it is possible to extract the transition energies in absolute terms. The new recoil corrected values are 987.9440 (5) keV and 1119.9335(14) keV. This results in new values for the excitation energies of the 3_1^- and 5_1^- levels with $E_{\mathrm{exc}}(3_1^-) = 1276.1315(12)$ keV and $E_{\mathrm{exc}}(5_1^-) = 1408.1205(15)$ keV. The energy difference of the two levels, $\Delta E = 131.9894(19)$ keV now has an uncertainty improved by almost an order of magnitude as compared to [10].

The increased solid angle of the bent crystal geometry of GAMS5 was needed for the search of the $5_1^- \rightarrow 3_1^-$ transition. The experiment was made as a relative measurement in terms of energy and intensity with respect to a reference line. Accordingly, it was sufficient to know the dispersion, i.e., the conversion of angle interferometer units (fringes) into wavelengths. The calibration was extracted from known (n, γ) lines of ^{36}Cl using perfect flat Si crystals with a known lattice spacing. The lattice constant of the curved Si crystals was determined using the same transitions. Both parameters undergo relative variations of less than 10^{-7} over several years. The total relative uncertainty of the dispersion relation is around 0.5×10^{-6}.

A $\sim$80 μm thin sample of 80 milligrams Gd_2O_3 powder isotopically enriched to 97% of ^{155}Gd was used. A small energy range of γ rays from 130 keV to 134 keV containing the 131.113(2) keV line as a reference was scanned for one week. The observed γ spectrum is shown in Fig. 3.

The most prominent line is the reference transition (R) at 131.119(3) keV. It is reported to have a γ intensity of 0.62 (4) per 10^4 captures [10]. The observed number of counts in this line is $N_\gamma(131.119) = 30718(308)$.

Another strong line is seen at 131.292(5) keV. This line (P) is an example of a so-called "parasitic" line. At a given Bragg angle, higher Bragg orders diffract higher energies producing parasitic peaks in lower-order spectra by the Compton background. In particular, the 262.585(4) keV line of ^{156}Gd produces a parasitic line with $N_\gamma(131.292) = 9307(244)$ counts. This can be compared to $N_\gamma(262.585) = 336261(1797)$ counts in the second order

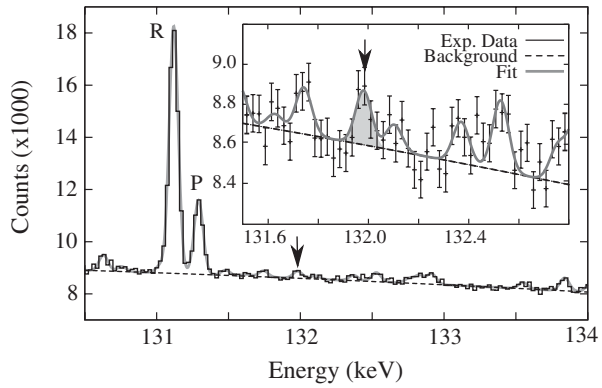

FIG. 3. A fragment of a γ spectrum from ^{155}Gd$(n_{\mathrm{th}}, \gamma)^{156}$Gd reaction measured with the GAMS5 spectrometer. The insert shows a zoom with the clearly identified $5^- \rightarrow 3^-$ transition. Other lines are described in the text.

spectrum showing that the second order reflex contains only a 0.028 fraction of counts in the first order.

The two prominent lines in the spectrum (R, P) provided a shape calibration for fitting weaker lines. One of the observed lines at 131.983(12) keV matches well the energy difference of $\Delta E = 131.9894(19)$ keV of the transition between the 5_1^- and 3_1^- levels. The observed number of counts is $N_\gamma(131.983) = 1031(132)$. We have checked up to the fifth order that this line does not correspond to a higher-order reflex of a different γ line. In the second order spectrum there is a line at 264.026(19) keV close to the double energy of the 131.983 keV. The number of counts in the 264.026 keV line is $N_\gamma(264.026) = 3528(312)$. Therefore, the corresponding parasitic peak at 132.013 keV, which cannot be resolved from the 131.983 keV line, contributes at most 99(10) counts. Hence, the corrected number of counts in the 131.983 keV line, $N_\gamma^C(131.983) = 932(133)$, determines the γ intensity of this line to be $1.9(3) \times 10^{-6}$ per neutron capture, when compared with the intensity of the reference line.

Table I summarizes properties of the relevant γ transitions in ^{156}Gd, published previously [9,10] and obtained in this work. As mentioned above, the critical signature for the existence of tetrahedral symmetry is the absence of intraband E2 transition matrix elements at the bottom of the negative-parity band [2]. Using the newly measured lifetime of the 5_1^- level at 1408.1205 keV and γ intensities shown in Table I, we could determine partial half-lives for the three decays from this level. The partial half-life for the 131.983 keV, $E2$ transition is $1.37^{+1.13}_{-0.24}$ ns and the corresponding $E2$ rate yields $B(E2, 131.983) = 293^{+61}_{-134}$ W.u. The $E1$ rates are $B(E1, 823.421) = (0.64^{+0.14}_{-0.29}) \times 10^{-3}$ W.u. and $B(E1, 1119.9335) = (0.85^{+0.19}_{-0.38}) \times 10^{-3}$ W.u..

Using the rotational formula $B(E2, I \rightarrow I-2) = (15/32\pi)e^2Q_0^2[(I-1)I/(2I-1)(2I+1)]$ we have determined the intrinsic quadrupole moment of the 5_1^-, 1408.1205 keV level in ^{156}Gd to be $Q_0 = 7.1^{+0.7}_{-1.6}$ b. The large value of this moment, which is comparable to the intrinsic quadrupole moment, $Q_0 = 6.83(37)$ b [23], of the ground state of ^{156}Gd, indicates a significant quadrupole collectivity in the disputed lowest odd-spin, negative-parity band in ^{156}Gd. It contradicts the presence of the tetrahedral symmetry in this band proposed in Refs. [1,2].

The new $B(E1)$ and $B(E2)$ rates for the decays from the 5_1^- level in ^{156}Gd are compared in Table II to the rates in the ground-state band of ^{156}Gd and to analogous $B(E1)$ and $B(E2)$ rates in the neighboring nuclei, ^{154}Sm, ^{154}Gd and ^{158}Gd. One can see that the $B(E\lambda)$ values obtained for ^{156}Gd are similar to those in the neighboring nuclei. We note in particular, that the $B(E\lambda)$ decay rates from the 5_1^- level in ^{158}Gd are very close to the corresponding rates in ^{156}Gd. With the rotational formula quoted above we obtained the intrinsic quadrupole moment of $Q_0 = 7.8^{+1.1}_{-1.7}$ b for the 5_1^- level in ^{158}Gd. This value compares well to the quadrupole moment, $Q_0 = 7.104(35)$ b [23] of the ground-state band in ^{158}Gd, indicating a strong quadrupole collectivity in the lowest odd-spin, negative-parity band, a behavior similar to that observed in this work for ^{156}Gd.

Following the criteria formulated in [1–4] the present work concludes that the negative parity band in ^{156}Gd is incompatible with a description based on tetrahedral symmetry. Therefore, future theoretical investigations should focus on the formulation of alternative criteria and/or the search for new test candidates.

[1] J. Dudek *et al.*, Phys. Rev. Lett. **88**, 252502 (2002).
[2] J. Dudek *et al.*, Phys. Rev. Lett. **97**, 072501 (2006).
[3] J. Dudek *et al.*, J. Phys. G **37**, 064032 (2010).
[4] A. Góźdź *et al.*, Int. J. Mod. Phys. E **19**, 621 (2010).
[5] Q. T. Doan *et al.*, Acta Phys. Pol. B**40**, 725 (2009).
[6] R. A. Bark *et al.*, Phys. Rev. Lett. **104**, 022501 (2010).
[7] J. Konijn *et al.*, Nucl. Phys. A **352**, 191 (1981).
[8] M. Sugawara *et al.*, Nucl. Phys. A **686**, 29 (2001).
[9] C. W. Reich, Nuclear Data Sheets **99**, 753 (2003).
[10] J. Klora *et al.*, Nucl. Phys. A **561**, 1 (1993).
[11] C. W. Reich, Nuclear Data Sheets **110**, 2257 (2009).
[12] R. G. Helmer, Nuclear Data Sheets **101**, 325 (2004).
[13] H. G. Börner *et al.*, Phys. Rev. C **59**, 2432 (1999).
[14] G. A. Leander *et al.*, Phys. Lett. B **152**, 284 (1985).
[15] W. R. Phillips *et al.*, Phys. Rev. Lett. **57**, 3257 (1986).
[16] W. Urban *et al.*, Phys. Lett. B **185**, 331 (1987).
[17] T. M. Shneidman *et al.*, Eur. Phys. J. A **25**, 387 (2005).
[18] ENSDF, www.nnds.bnl.gov, January 2010.
[19] P. D. Cottle and N. V. Zamfir, Phys. Rev. C **54**, 176 (1996).
[20] E. G. Kessler *et al.*, Nucl. Instrum. Methods Phys. Res., Sect. A **457**, 187 (2001).
[21] H. G. Börner *et al.*, J. Phys. G **19**, 217 (1993).
[22] M. Jentschel *et al.*, J. Res. Natl. Inst. Stand. Technol. **105**, 25 (2000).
[23] S. Raman *et al.*, At. Data Nucl. Data Tables **36**, 1 (1987).